

A universal automated tool for reliable detection of seizures in rodent models of acquired and genetic epilepsy

Pablo M. Casillas-Espinosa^{1,2} | Armen Sargsyan³ | Dmitri Melkonian³ |

Terence J. O'Brien^{1,2,4,5}

¹Departments of Neuroscience and Medicine, Central Clinical School, Monash University, Melbourne, Victoria, Australia

²Department of Medicine, Royal Melbourne Hospital, University of Melbourne, Melbourne, Victoria, Australia

³KaosKey, Sydney, New South Wales, Australia

⁴Department of Neurology, Alfred Hospital, Melbourne, Victoria, Australia

⁵Department of Neurology, Royal Melbourne Hospital, Parkville, Victoria, Australia

Correspondence

Terence J. O'Brien, Department of Neuroscience, Central Clinical School, Monash University, Melbourne, VIC, Australia.

Email: terence.obrien@monash.edu

Summary

Objective: Prolonged electroencephalographic (EEG) monitoring in chronic epilepsy rodent models has become an important tool in preclinical drug development of new therapies, in particular those for antiepileptogenesis, disease modification, and treating drug-resistant epilepsy. We have developed an easy-to-use, reliable, computational tool for automated detection of electrographic seizures from prolonged EEG recordings in rodent models of epilepsy.

Methods: We applied a novel method based on advanced time-frequency analysis that detects EEG episodes with excessive activity in certain frequency bands. The method uses an innovative technique of short-term spectral analysis, the Similar Basis Function algorithm. The method was applied for offline seizure detection from long-term EEG recordings from four spontaneously seizing, chronic epilepsy rat models: the fluid percussion injury (n = 5 rats, n = 49 seizures) and post–status epilepticus models (n = 119 rats, n = 993 seizures) of acquired epilepsy, and two genetic models of absence epilepsy, Genetic Absence Epilepsy Rats from Strasbourg and Wistar Albino Glaxo from Rijswijk (n = 41 and 14 rats, n = 8733 and 825 seizures, respectively).

Results: Our comparative analysis revealed that the EEG amplitude spectra of these four rat models are remarkably similar during epileptiform activity and have a single expressed peak within the 17- to 25-Hz frequency range. Focusing on this band, our computer program detected all seizures in the 179 rats. A quick semiautomated user inspection of the EEGs for the period of each identified event allowed quick rejection of artifact events. The overall processing time for 12-day-long recordings varied from a few minutes (5–10) to 30 minutes, depending on the number of artifact events, which was strongly correlated with the signal quality of the raw EEG data.

Significance: Our automated seizure detection tool provides high sensitivity, with acceptable specificity, for long- and short-term EEG recordings from both acquired and genetic chronic epilepsy rat models. This tool has the potential to improve the efficiency and rigor of preclinical research and therapy development using these models.

P.M.C.-E. and A.S. contributed equally to this work.

KEYWORDS

automated seizure detection, genetic absence epilepsy rats from Strasbourg, post–status epilepticus model, posttraumatic epilepsy, traumatic brain injury, Wistar Albino Glaxo from Rijswijk

1 | INTRODUCTION

Epilepsy affects 50 million people worldwide (World Health Organization, 2006), and poses a significant burden on the quality of life of affected individuals and their families. Since the discovery of bromide as the first antiseizure drug, there has been an impressive expansion of clinically effective therapies that decrease the frequency and severity of seizures in people with epilepsy. The newer antiseizure drugs have been identified through systematic screening in batteries of an increasing number of *in vivo* and *in vitro* seizure and epilepsy models.¹

However, the focus of translational research and drug development for the epilepsies has now shifted from the development of more antiseizure drugs to the development of antiepileptogenic and disease-modifying therapies. Prolonged electroencephalographic (EEG) recordings in chronic epilepsy models are a critical part of the drug development testing paradigm for these therapies.^{2–6} For this, an efficient and accurate measure of quantitating the occurrence of spontaneous seizures is critical.^{3,7}

For the study of acquired epilepsy, the two most common used models are the post–status epilepticus (SE) model⁶ and the traumatic brain injury–induced posttraumatic epilepsy (PTE) models.⁸ Conversely, Genetic Absence Epilepsy Rats from Strasbourg (GAERS) and Wistar Albino Glaxo from Rijswijk (WAG/Rij) are the most widely used models to study genetic generalized epilepsy with absence seizures.^{4,5} Prolonged EEG monitoring is necessary to phenotype the occurrence of spontaneous seizures in different animal models and to evaluate the acute and chronic effects of the novel interventions.⁹ Studies utilizing EEG typically involve comparison of measurements obtained from different experimental groups or from the same experimental group at different times. Given the heterogeneity of epilepsy and, in some cases, the low frequency of spontaneously occurring seizures, to appropriately power antiepileptogenesis and disease modification studies, it is mandatory to have a large number of animals per cohort as well as multiple and prolonged periods of recording to establish whether the experimental treatments are successful in preventing or modifying the progression of epilepsy.^{2,3,7,9}

Therefore, it is critical to quantify the presence and number of seizures in preclinical studies. Although EEG seizures can be relatively easy to recognize during expert visual

Key Points

- The “Assyst” novel and versatile algorithm detected 100% of 10 600 seizures, which represents >76 000 hours of EEG recordings
- We discovered a frequency band of 17–25 Hz that is specific to detect all of the seizures in the post-SE, post-TBI, GAERS, and WAG/Rij rodent models of acquired and genetic epilepsy
- Processing and reviewing 24 hours of EEG recordings took an average of 1 minute per 24 hours of EEG recordings, which represents saving 90%–98% of the time it takes to review preclinical EEG

inspection of the EEG, the overall process to analyze EEG recordings is very time-consuming. Moreover, it requires a significant amount of time to train a new EEG reviewer, and the manual analysis is prone to errors mostly related to fatigue and eyestrain. Thus, an automatic seizure detection method would greatly increase the throughput and would help to standardize and increase the reproducibility of the analysis in large-scale preclinical trials.

Here, we report a user-friendly, easy-to-use, reliable, computational tool for detection of EEG seizures from prolonged EEG recordings in rodent models of epilepsy, and validate this in prolonged EEG recordings from four rat models of chronic epilepsy, two acquired and two genetic. The tool is based on a novel signature in the 17- to 25-Hz frequency band of the EEG that is specific to detect all of the EEG seizures in these four rodent models.

2 | MATERIALS AND METHODS

2.1 | Animals

Eleven-week-old male Wistar rats were used for the post-SE and PTE models of acquired epilepsy (at the time of application of the epileptogenic insult). Twenty-four-week-old male GAERS and WAG/Rij rats were used in the experiments. All procedures were approved by the Florey Animal Ethics Committee (ethics number 14-072 UM). The animals were individually housed with alternating 12-hour light and dark cycles. Food and water were provided *ad libitum* for the whole duration of the study.

2.2 | Kainic acid–induced post-SE model of acquired epilepsy

A repeated low-dose kainic acid (KA) administration protocol was used as previously described.¹⁰ Rats were injected intraperitoneally (i.p.) with an initial dose of KA 7.5 mg/kg. Animals were monitored for behavioral seizures based on the Racine scale.^{11,12} If no self-sustained seizure activity was observed with at least five class IV-V seizures per Racine, another i.p. dose of 2.5 mg/kg of KA was administered up to a maximum of 15 mg/kg. An animal was eliminated from the experiment if it did not show a self-sustained SE after a maximum KA dose. SE was stopped after 4 hours with diazepam (5 mg/kg/dose). After recovery, the animals were returned to their home cages in the animal house and kept in routine housing conditions until they were implanted with EEG electrodes for the prolonged EEG recordings (as described below).

2.3 | Induction of PTE

Wistar rats received a lateral fluid percussion injury (FPI) as previously described.^{8,13} Briefly, with the animal under anesthesia, a 5-mm craniotomy positioned 4 mm right lateral and 4 mm posterior to bregma was performed to create a circular window exposing the intact dura mater of the brain. A modified female Luer-Lock cap was secured over the craniotomy window by dental acrylic. A severe intensity (320–350 kPa) fluid pulse of silicone oil generated by the fluid percussion device was delivered to the brain. On resumption of spontaneous breathing, and return to pre-FPI levels of heart rate and oxygenation status, the dental acrylic caps were removed and the wound was sutured closed. This injury results in PTE in 30%–50% of rats at 6 months.^{8,13–16} After recovery, the animals were returned to their home cages in the animal house and kept in routine housing conditions until they were implanted with EEG electrodes for the prolonged EEG recordings (as described below).

2.4 | EEG electrode implantation surgery

Surgery was performed 6 weeks after SE or FPI, or at 6 months of age for the GAERS and WAG/Rij, as previously described.¹⁷ Briefly, animals were anesthetized with isoflurane. Six burr holes were drilled through the skull without penetrating the dura, one on each side anterior to the bregma, two to each side anterior to lambda, and two to each side in the parietal bones. Ground and reference electrodes were placed in the occipital bone. Stainless steel subdural screw recording electrodes (Plastics One) were screwed into each hole. The recording electrodes were fixed in position by applying Vertex dental cement around the electrodes and over the skull.

2.5 | EEG recordings

EEG was acquired using Profusion 5 software (Compumedics) unfiltered and digitized at 512 Hz using a tethered EEG cable system with the rats freely moving in their home cages. EEG recordings were acquired for 2–4 weeks continuously in the post-SE and FPI rats, whereas GAERS and WAG/Rij had 48 hours of continuous EEG recordings. Only animals that presented with EEG seizures on the EEG were selected for the study. A referential montage was used.

2.6 | Manual seizure analysis

EEG analysis was performed in a blinded manner and confirmed by two different expert observers. All EEG recordings were visually and manually annotated using Profusion 5 software. For the post-SE and PTE animals, an EEG seizure was defined as an episode of rhythmic spiking activity that was three times the baseline amplitude with a frequency > 5 Hz lasting at least 10 seconds. The end of a seizure was determined as the last spike.^{16,18,19}

For GAERS and WAG/Rij, an EEG seizure was defined as spike and wave discharge (SWD) of amplitude of more than three times baseline, a frequency of 7–12 Hz, and duration of >0.5 seconds.^{4,5,20,21} The start and end of each seizure was determined by manually marking the beginning and end of each SWD on the EEG. For all of the animals, the total number of seizures was quantified.

2.7 | Automated seizure analysis

We developed a novel software tool, “Assyst,” written in Delphi (dialect of Object Pascal, Embarcadero Technologies), that is intended to significantly facilitate the detection of electrographic seizures in prolonged EEG recordings in rodent models of epilepsy. The seizure detection method implemented in Assyst and presented here utilizes an advanced time-frequency analysis of the signal from a single or multiple EEG channels to reveal the EEG segments with excessive activity in a certain frequency band. We assessed the spectral content of the EEG within a given frequency band using a measure we refer to as spectral band index (SBI), which we calculate over time using a predetermined running time window.

The main steps of the algorithm are presented in Figure 1. The algorithm consists of main (shaded blocks) and optional (white blocks) steps. The proposed algorithm is interactive; some operations are automatically performed by the computer, others require user input.

2.8 | Input data

EEG recordings are exported unfiltered into European data format (.edf) files and then are loaded to the Assyst software.

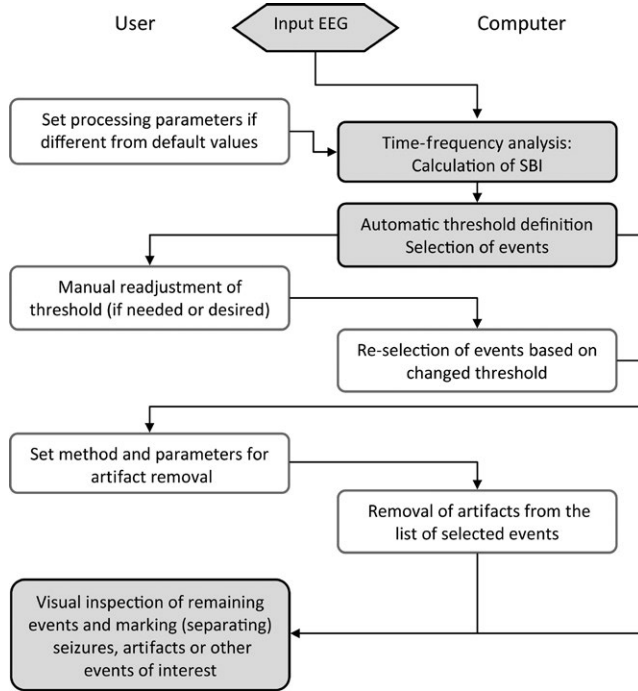


FIGURE 1 Block diagram of the algorithm. Shaded blocks indicate main steps; white blocks indicate optional steps. The blocks on the left side indicate operations performed by the user, and blocks on the right side those performed by the computer. EEG, electroencephalogram; SBI, spectral band index

There are no restrictions on the duration of the EEG recordings, data size, or number of channels to be analyzed.

2.9 | Time-frequency analysis—calculation of SBI

This step is intended to reveal the temporal dynamics of a particular frequency component of the EEG. To achieve this, we define the frequency range of interest, (frequency band), define the length of EEG segments (time window) that will be used to calculate the power spectrum of the EEG, and move this window along the EEG with certain time step. For each window position (Figure 2), the power spectrum of the EEG segment is calculated within the defined frequency range using a modification of our Similar Basis Function (SBF) algorithm for Fourier Transform.²² The maximum value of the power spectrum in this frequency range is found, and this parameter—the SBI—is used as an estimate for spectral intensity of the EEG within this frequency band. The SBI values are then plotted against time at centers of consecutive windows to form the SBI curve (Figure 2).

2.10 | Event selector

To find the times of high electrical EEG activity suggestive of seizures within the frequency band of interest, we define a

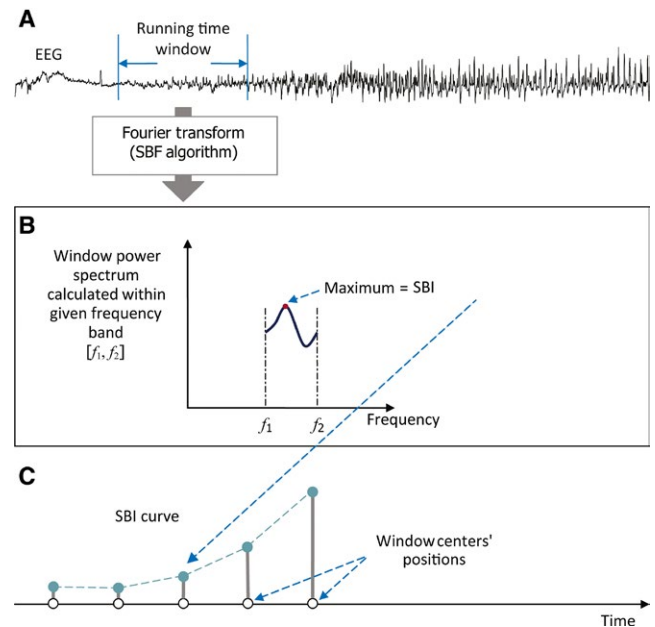


FIGURE 2 Diagram showing calculation of spectral band index (SBI) curve. A, Fragment of electroencephalogram (EEG) and the current position of running time window. B, The Fourier transform and the power spectrum of EEG segment from this window are calculated using the Similar Basis Function algorithm, for the frequency range $[f_1, f_2]$. The maximum value of the power spectrum in this range is the SBI of the current window. C, The SBIs of consecutive time windows are then plotted against time and form the SBI curve

threshold value of the SBI. This threshold allows filtering background EEG signal and interictal activity from the seizures. The automatic threshold definition is based on building a distribution histogram of SBI values over the entire recording time (Data S1). Assuming that the total duration of ictal events is only a small fraction of overall duration of the recording, the region of the histogram with the highest density of distribution will indicate the interictal SBI value range. By setting the threshold above this range, we will cut off the “ordinary” values of the SBI and leave only the seizure events (Figure S1).

After the threshold is defined, all episodes of the EEG for which the SBI is above the threshold are separated in a list of events that also specifies their start and end times.

If multiple channels are analyzed, the algorithm groups the overlapping events from different channels, so they can be counted as one event. The start and end times of the selected events are roughly determined as the points where the SBI curve crosses the threshold (Figure S1). The precision of defining the starts and ends in this way is equal to the size of the time window. However, the software allows the user to redefine the start and end times of selected events manually, simply moving special cursors to desired positions on the EEG. The Assyst software is able to show the signal of single or multiple channels to provide the user a more efficient review of the events.

TABLE 1 Total number of seizures analyzed

Model	Animals, n	Events, n					
		Manually annotated by expert	Automatically selected by event selector	Removed by artifact removal procedure	Rejected by the user	Classified as seizures by the user	Verified by two independent experts
Post-SE	119	989	32 877	13 204	18 680	993	993
PTE	5	43	1538	171	1318	49	49
GAERS	41	8733	9412	Not applied	679	8733	8733
WAG/Rij	14	825	856	Not applied	31	825	825
Total	179	10 590	44 683	13 375	20 708	10 600	10 600

GAERS, Genetic Absence Epilepsy Rats from Strasbourg; PTE, posttraumatic epilepsy; SE, status epilepticus; WAG/Rij, Wistar Albino Glaxo from Rijswijk.

2.11 | Artifact removal and user inspection of selected events

An optional automatic artifact removal procedure in our method identifies and eliminates false-positives (FPs) that were caused by strong artifacts. It is performed after the threshold-based event selection. The procedure examines the selected events for the presence of sharp artifacts by analyzing the signal's derivative and finding the pieces of EEG with sharp and large deflections in amplitude (Data S3).

The final stage of processing requires the input from the user. At this stage, the user visually examines the selected events by reviewing the EEG either to confirm them as electrographic seizures or reject them as false detections.

2.12 | Comparison of Assyst and manual seizure detection and algorithm performance assessment

All of the EEG recordings were manually analyzed as described previously by two blinded experts. Assyst software was used to analyze the same EEG recordings and the results obtained by Assyst were confirmed by two independent blinded reviewers. The total number of EEG seizures detected by each method and the time to review each file were analyzed. The main criterion for the algorithm performance assessment was the percentage of real seizures detected by the algorithm during the automatic event detection (sensitivity).

The second criterion was the comparison of total time spent for the analysis of 1 day (24 hours) of recording using the Assyst software.

3 | RESULTS

3.1 | Automated seizure detection

The method was applied for offline EEG seizure detection from long-term EEG recordings from post-SE, PTE, GAERS, and WAG/Rij models. We processed recordings from 179 rats that were representatives of four different rat models of epilepsy. The EEG recordings contained in total 10 600 seizures, which represents >76 000 hours of EEG recordings (Table 1). The average duration of records from post-SE and PTE animals was 24.6 days. The records from GAERS and WAG/Rij animals were shorter and averaged 24.2 hours (± 3.4 hours).

For post-SE ($n = 119$ rats, $n = 993$ seizures, 2.8 seizures per week) and PTE ($n = 5$ rats, $n = 49$ seizures, 28 seizures per week), the EEG seizure detection was performed using the following sets of parameters. The running window size was 10 seconds, the window step was 5 seconds, and the frequency band was from 20 to 23 Hz.

For GAERS ($n = 41$, $n = 8733$ seizures) and WAG/Rij ($n = 14$ rats, $n = 825$ seizures), the parameters for automated

seizure detection were slightly different. We used shorter windows, 2-5 seconds for GAERS and 5 seconds for WAG/Rij, to reliably detect the shorter SWD of these genetically inbred species. The window step was equal to half of the window size. Also, the EEG seizures in both the GAERS and WAG/Rij rats showed slightly higher variability in the frequency of the component we were focusing on (Figure S2), and thus a wider frequency band of 17-25 Hz was used in the SBI calculation.

Examples of electrographic seizures in post-SE, PTE, GAERS, and WAG/Rij models are shown in Figure 3. Note that the average discharge frequency (the repetition rate of spikes) significantly differs between the models: 6 Hz for post-SE, 2.4 Hz for PTE, 7.3 Hz for GAERS, and 9 Hz for WAG/Rij. Meanwhile, the waveforms of individual spike waves from different rat models (Figure 3B) have similar structure and temporal dynamics. Due to this temporal similarity, they also have similar amplitude-frequency characteristics, with a single peak in the range 17-25 Hz (Figure S2).

Figure 4 illustrates the specificity of the 17- to 25-Hz frequency component to EEG seizures. This narrow band shows a significant difference between SBI values corresponding to ictal events and those corresponding to background interictal activity. It is important to note that the smallest ictal SBI

value is >10 times larger than the largest interictal SBI value, which provides a very safe margin for threshold to detect seizures.

In Data S2, we compare and discuss the SBI curves calculated for the same recording for wide and narrow frequency bands (Figure S3).

3.2 | Artifact removal

The majority of analyzed records contained artifacts. The optional procedure for automatic identification and removal of detections caused by artifacts was performed after the initial threshold-based event selection. A conservative removal algorithm was applied to avoid erroneous removal of ictal events (Data S3 and Figures S4-S5).

It is important to note that the number of true seizures detected with our algorithm does not depend on the use of the artifact removal tool. Rather, the artifact removal reduces the FP rate and the time it takes to manually review the selected events. In all of the post-SE and PTE recordings, the automatic artifact removal procedure removed on average 38.5% of the artifacts that were initially selected by the algorithm.

In post-SE and PTE EEG recordings that did not contain artifacts ($n = 7$) or contained a few (Figures 4 and S3), the number of FPs was zero. In these cases, the specificity of the algorithm with or without the use of the artifact removal procedure was 100%.

The EEG recordings from GAERS and WAG/Rij rats contained only a minimal number of artifacts, and the artifact removal procedure was not used.

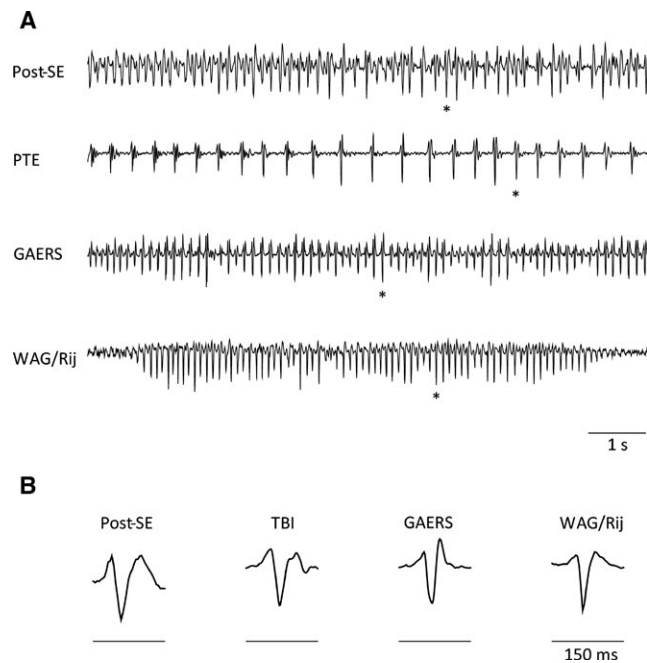


FIGURE 3 A, Examples of electrographic seizures (10-second fragments) from four rat models. B, One hundred fifty-millisecond fragments of traces in A showing single spike waves (marked by asterisk in corresponding trace in A). GAERS, Genetic Absence Epilepsy Rats from Strasbourg; PTE, posttraumatic epilepsy; SE, status epilepticus; TBI, traumatic brain injury; WAG/Rij, Wistar Albino Glaxo from Rijswijk

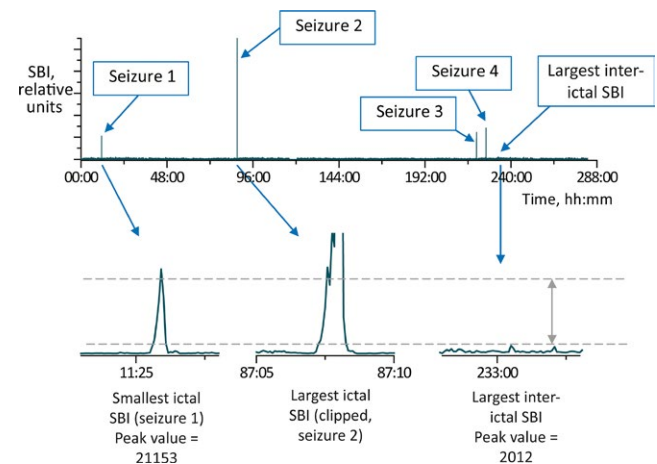


FIGURE 4 Narrowband seizure detection. Upper trace shows the spectral band index (SBI) curve calculated for a 12-day (288 hours) electroencephalographic recording from a post-status epilepticus rat that had four seizures during the recording period. The bottom traces show zoomed fragments of the SBI curve corresponding to the first and second seizures that have the smallest and the largest SBI values, correspondingly, among all ictal events, and the interictal event with the largest SBI value. The SBI peak values are in relative units

3.3 | Algorithm performance assessment

We assessed the algorithm performance using two criteria: sensitivity (the percentage of real seizures detected by the algorithm) and time-saving compared to manual seizure screening.

For all analyzed records, the comparison of the EEG seizures detected with the use of Assyst software with the previous manual scores made by experts did not reveal any missed seizures (0 false-negatives), that is, the program detected 100% of EEG seizures in all records. This was verified afterward by two independent experts (Table 1). Moreover, it was revealed that four seizures in the post-SE animals and six seizures in PTE animals were not annotated in the manual analysis. The FP rate was not affected by the duration of the EEG recordings.

Assyst significantly reduced the time to screen for seizures in EEG recordings. The longest time spent by processing a single channel EEG recording of one animal was about 5 minutes per 1 day of record, with an average of 1 minute per 24 hours of EEG recordings (Table 2). For post-SE and PTE recordings that contained minimal artifacts, the processing took about 6-10 seconds per day of recording. As expected, longer inspection time was required for GAERS and WAG/Rij records, as each record contained hundreds of seizures per 24 hours of EEG recordings.

In contrast, an experienced investigator spends 40-90 minutes for manual seizure screening through 1 day of EEG recordings. Comparing our average Assyst processing time with the manual seizure screening, the time needed to screen for seizures in any given set of EEG recordings was reduced by 60 times, which represents saving 90%-98% of the time needed by the reviewer when using the Assyst.

4 | DISCUSSION

We present an effective and efficient automated algorithm that has high sensitivity, detecting all of the seizures in different chronic animal models of genetic and acquired epilepsy in this study, and high specificity, with only a small, acceptable, number of FP seizure identifications. The Assyst method

TABLE 2 Processing times of 24 hours of EEG recordings

	Processing time per 1 day of EEG recordings	
		Minutes
Assyst	Max	5
	Min	0.1
	Average	1
Manual ^a		40-90

EEG, electroencephalographic.

^aApproximate time spent by expert for visual examination of 1 day of EEG recordings.

was applied for offline seizure detection from long-term EEG recordings from four spontaneously seizing, chronic epileptic rat models: the post-SE model of acquired epilepsy, the FPI model of PTE, and two genetic models of absence epilepsy, GAERS and WAG/Rij.

Seizure detection algorithms have been described in the literature,^{23,24} most of which are aimed at human EEG analysis; very few are designed particularly for rodents.²⁵⁻³⁴ However, no method has been described to detect all of the seizures in different animal models.

The method presented here belongs to the class of univariate time-frequency analysis-based methods. The novelty is in the definition and in the way of calculation of the discriminative feature used—the SBI, which is calculated for a narrow frequency band and is used to assess the spectral content of the EEG to distinguish the EEG seizures from interictal activity.

We found that the ictal EEG in the examined rat models contains a strong component in the frequency range from 17 to 25 Hz. This novel finding was critical to determine the choice for the discriminative feature of EEG seizures and ensured an effective performance of the algorithm. We found that this peculiarity comes from the frequency composition of single discharges, or individual spike and wave complexes within the seizures in these animals (Data S2, Figure S2). Importantly, this frequency band component is not present anywhere else in the interictal EEG. This is reflected in that the power spectrum of the EEG (and the SBI) has much stronger values in this frequency range during the seizures than at any time between seizures (Figure 4).

Another key factor for the algorithm's performance was the accuracy of calculation of the power spectrum achieved by using our previously described SBF algorithm for numerical calculations of Fourier transforms.²² Numerical estimation of Fourier transforms is usually based on procedures employing various algorithms of the fast Fourier transform (FFT).³⁵ The latter is supported by a Fourier series model of the data, that is, the addressees are periodic signals. This distinction with the Fourier integrals is a troublesome problem when functions of short duration, like EEG fragments extracted by employed windows, are transformed from the time to frequency domain. The major concern is the spectral leakage, which may cause significant distortions of the frequency domain characteristics. The remedies of windowing and zero-padding usually introduce problems of their own. By contrast to the FFT, the SBF algorithm is an original version of Filon-type methods that provide maximum precision in the estimation of trigonometric integrals using interpolation polynomials of different degrees. Removal of spectral leakage provides a means to calculate the power spectrum with high resolution and remarkable accuracy.

In this study, we used a modified SBF algorithm optimized for calculation of uniformly sampled input signal,

which is the case for EEG recordings. This optimization made the algorithm significantly faster and comparable in speed with the FFT.

Current implementation of the algorithm is not devoted to real-time EEG processing because the threshold is defined on the basis of the entire record. Implementation of some offline procedures was necessary to get the most accurate (for each particular recording) statistical estimate for the baseline SBI values. Using these results, we are currently working on the online version of the algorithm, where the threshold will be defined dynamically based on the past values of SBI.

The majority of our records contained artifacts, both of physiological and nonphysiological (instrumental) nature. Most physiological artifacts did not have strong components in the analyzed frequency band, and thus were rarely detected by the algorithm, with the exception of strong electrocardiographic or chewing artifacts (Figure S4A,B). In contrast, the nonphysiological artifacts were sometimes detected as events of interest because they mostly contain sharp and large amplitude signal that has strong spectral power within a wide frequency diapason including the 17- to 25-Hz band (Figure S4C-F).

A variety of artifact detection and removal methods of different complexity are described in literature, although no single existing artifact detection method is universal. Importantly, there is no method designed specifically for single-channel recordings in rodents.^{36,37}

When artifact identification is applied in a seizure detection algorithm, there is a high risk of erroneously identifying a seizure as an artifact, especially if the seizure is contaminated by artifacts, as occurs normally in chronic EEG recordings and we observed several times in our recordings.³⁸ Therefore, we decided to use a reliable and conservative procedure for artifact identification. This procedure did not erroneously remove any seizure in the studied records, and further reduced the user's inspection time on average by about 40%.

False-negatives are the most critical component for a reliable automated seizure detection method. One missed seizure during the automated detection would require a manual inspection of the entirety of the EEG recording file.

In our case, the sensitivity was 100% (ie, zero false-negatives) in all records from all four epilepsy rat models. Specificity, which is determined by the number of FPs, significantly depended on the quality of recording. In recordings with a reduced number of artifacts, the number of FPs was zero, giving specificity of 100%.

In records containing a large number of artifacts even after application of an artifact removal procedure, the number of FPs remaining for visual inspection was relatively high (ranging from 0 to 193/d, on average 32/d, or 1.3/h), which is comparable to what has been described in the literature.^{38,39}

Overall, we have shown a reliable automated tool that provides high sensitivity, detecting 100% of the EEG seizures in different animal models of genetic and acquired epilepsy. Our Assyst is versatile and a significantly time-saving seizure detection program, which can facilitate high-throughput studies. Moreover, it provides remarkable flexibility in processing depending on particular data and user needs, from automatic with minimum influence from the user to a semi-automated inspection of every peak, large or small. Moreover, the software provides flexibility to advanced users to search for epileptiform events with smaller duration and amplitude or when dealing with new or uncharacterized models. The Assyst algorithm has the potential to improve the efficiency and rigor of preclinical research and therapy development using these models.

ACKNOWLEDGMENTS

We thank Prof Gilles van Luijelaar (Radboud University Nijmegen, the Netherlands) for kindly providing the WAG/Rij rat data.

DISCLOSURE

None of the authors has any conflict of interest to disclose. We confirm that we have read the Journal's position on issues involved in ethical publication and affirm that this report is consistent with those guidelines.

REFERENCES

1. Galanopoulou AS, Buckmaster PS, Staley KJ, et al. Identification of new epilepsy treatments: issues in preclinical methodology. *Epilepsia*. 2012;53:571–82.
2. Barker Haliski M, Friedman D, French J, et al. Disease modification in epilepsy: from animal models to clinical applications. *Drugs*. 2015;75:749–67.
3. Galanopoulou A, Mowrey W. Not all that glitters is gold: a guide to critical appraisal of animal drug trials in epilepsy. *Epilepsia Open*. 2016;1:86–101.
4. Coenen AM, Drinkenburg WH, Inoue M, et al. Genetic models of absence epilepsy, with emphasis on the WAG/Rij strain of rats. *Epilepsy Res*. 1992;12:75–86.
5. Marescaux C, Vergnes M, Depaulis A. Genetic absence epilepsy in rats from Strasbourg—a review. *J Neural Transm Suppl*. 1992;35:37–69.
6. Morimoto K, Fahnestock M, Racine RJ. Kindling and status epilepticus models of epilepsy: rewiring the brain. *Prog Neurobiol*. 2004;73:1–60.
7. Galanopoulou AS, Simonato M, French JA, et al. Joint AES/ILAE translational workshop to optimize preclinical epilepsy research. *Epilepsia*. 2013;54(Suppl 4):1–2.
8. Liu S-J, Zheng P, Wright D, et al. Sodium selenate retards epileptogenesis in acquired epilepsy models reversing changes in protein phosphatase 2A and hyperphosphorylated tau. *Brain*. 2016;139:1919–38.

9. Kadam S, D'Ambrosio R, Duveau V, et al. Methodological standards and interpretation of video-electroencephalography in adult control rodents. A TASK1-WG1 report of the AES/ILAE translational Task Force of the ILAE. *Epilepsia*. 2017;58(Suppl 4):10–27.
10. Bhandare A, Kapoor K, Powell K, et al. Inhibition of microglial activation with minocycline at the intrathecal level attenuates sympathoexcitatory and proarrhythmogenic changes in rats with chronic temporal lobe epilepsy. *Neuroscience*. 2017;350:23–38.
11. Racine RJ. Modification of seizure activity by electrical stimulation: I. After-discharge threshold. *Electroencephalogr Clin Neurophysiol*. 1972;32:269–79.
12. Racine RJ. Modification of seizure activity by electrical stimulation II. Motor seizure. *Electroencephalogr Clin Neurophysiol*. 1972;32:281–94.
13. Shultz SR, Wright DK, Zheng P, et al. Sodium selenate reduces hyperphosphorylated tau and improves outcomes after traumatic brain injury. *Brain*. 2015;138:1297–313.
14. Kharatishvili I, Nissinen JP, McIntosh TK, et al. A model of post-traumatic epilepsy induced by lateral fluid-percussion brain injury in rats. *Neuroscience*. 2006;140:685–97.
15. Shultz SR, Cardamone L, Liu YR, et al. Can structural or functional changes following traumatic brain injury in the rat predict epileptic outcome? *Epilepsia*. 2013;54:1240–50.
16. Brady R, Casillas Espinosa P, Agoston D, et al. Modelling traumatic brain injury and posttraumatic epilepsy in rodents. *Neurobiol Dis*. 2018;123:8–19.
17. Casillas Espinosa P, Powell K, Zhu M, et al. Evaluating whole genome sequence data from the Genetic Absence Epilepsy Rat from Strasbourg and its related non-epileptic strain. *PLoS One*. 2017;12:e0179924.
18. Van Nieuwenhuysse B, Raedt R, Sprengers M, et al. The systemic kainic acid rat model of temporal lobe epilepsy: long-term EEG monitoring. *Brain Res*. 2015;1627:1–11.
19. Pitkänen A, Kharatishvili I, Narkilahti S, et al. Administration of diazepam during status epilepticus reduces development and severity of epilepsy in rat. *Epilepsy Res*. 2005;63:27–42.
20. Powell KL, Cain SM, Ng C, et al. A Cav3.2 T-type calcium channel point mutation has splice-variant-specific effects on function and segregates with seizure expression in a polygenic rat model of absence epilepsy. *J Neurosci*. 2009;29:371–80.
21. Drinkenburg WH, Coenen AM, Vossen JM, et al. Spike-wave discharges and sleep-wake states in rats with absence epilepsy. *Epilepsy Res*. 1991;9:218–24.
22. Melkonian D. Similar basis function algorithm for numerical estimation of Fourier integrals. *Numer Algorithms*. 2010;54:73–100.
23. Koren J, Herta J, Fürbass F, et al. Automated long-term EEG review: fast and precise analysis in critical care patients. *Front Neurol*. 2018;9:454.
24. Ulate Campos A, Coughlin F, Gaínza Lein M, et al. Automated seizure detection systems and their effectiveness for each type of seizure. *Seizure*. 2016;40:88–101.
25. Xanthopoulos P, Liu C-C, Zhang J, et al. A robust spike and wave algorithm for detecting seizures in a genetic absence seizure model. *Conf Proc IEEE Eng Med Biol Soc*. 2009;2009:2184–7.
26. van Luijckelaar G, Lüttjohann A, Makarov V, et al. Methods of automated absence seizure detection, interference by stimulation, and possibilities for prediction in genetic absence models. *J Neurosci Methods*. 2016;260:144–58.
27. Ovchinnikov A, Lüttjohann A, Hramov A, et al. An algorithm for real-time detection of spike-wave discharges in rodents. *J Neurosci Methods*. 2010;194:172–8.
28. Aghazadeh R, Shahabi P, Frounchi J, et al. An autonomous real-time single-channel detection of absence seizures in WAG/Rij rats. *Gen Physiol Biophys*. 2015;34:285–91.
29. Van Hese P, Martens JP, Boon P, et al. Detection of spike and wave discharges in the cortical EEG of genetic absence epilepsy rats from Strasbourg. *Phys Med Biol*. 2003;48:1685–700.
30. Richard CD, Tanenbaum A, Audit B, et al. SWDreader: a wavelet-based algorithm using spectral phase to characterize spike-wave morphological variation in genetic models of absence epilepsy. *J Neurosci Methods*. 2015;242:127–40.
31. White A, Williams P, Hellier J, et al. EEG spike activity precedes epilepsy after kainate-induced status epilepticus. *Epilepsia*. 2010;51:371–83.
32. Niknazar M, Mousavi SR, Motaghi S, et al. A unified approach for detection of induced epileptic seizures in rats using ECoG signals. *Epilepsy Behav*. 2013;27:355–64.
33. Lee J, Park J, Yang S, et al. Early seizure detection by applying frequency-based algorithm derived from the principal component analysis. *Front Neuroinform*. 2017;11:52.
34. Dheer P, Chaitanya G, Pizarro D, et al. Seizure detection and network dynamics of generalized convulsive seizures: towards rational designing of closed-loop neuromodulation. *Neurosci J*. 2017;2017:9606213.
35. Rao KR, Kim DN, Hwang JJ. Fast Fourier transform: algorithms and applications. Dordrecht, the Netherlands and Heidelberg, Germany: Springer; 2010.
36. Islam M, Rastegarnia A, Yang Z. Methods for artifact detection and removal from scalp EEG: a review. *Neurophysiol Clin*. 2016;46:287–305.
37. Islam M, Rastegarnia A, Yang Z. A wavelet-based artifact reduction from scalp EEG for epileptic seizure detection. *IEEE J Biomed Health Inform*. 2016;20:1321–32.
38. White A, Williams P, Ferraro D, et al. Efficient unsupervised algorithms for the detection of seizures in continuous EEG recordings from rats after brain injury. *J Neurosci Methods*. 2006;152:255–66.
39. Andrade P, Paananen T, Cizek R, et al. Algorithm for automatic detection of spontaneous seizures in rats with post-traumatic epilepsy. *J Neurosci Methods*. 2018;307:37–45.

SUPPORTING INFORMATION

Additional supporting information may be found online in the Supporting Information section at the end of the article.

How to cite this article: Casillas-Espinosa PM, Sargsyan A, Melkonian D, O'Brien TJ. A universal automated tool for reliable detection of seizures in rodent models of acquired and genetic epilepsy. *Epilepsia*. 2019;00:1–9. <https://doi.org/10.1111/epi.14691>